Modeling crowd turbulence by many-particle simulations

Wenjian Yu and Anders Johansson
Institute for Transport & Economics, Dresden University of Technology, Andreas-Schubert Strasse 23, 01062 Dresden, Germany
and Department of Humanities and Social Sciences, ETH Zurich, UNO D 11 Universitätstrasse 41, 8092 Zurich, Switzerland
(Received 30 May 2007; revised manuscript received 21 July 2007; published 10 October 2007)

A recent study [D. Helbing, A. Johansson, and H. Z. Al-Abideen, Phys. Rev. E **75**, 046109 (2007)] has revealed a "turbulent" state of pedestrian flows, which is characterized by sudden displacements and causes the falling and trampling of people. However, turbulent crowd motion is not reproduced well by current many-particle models due to their insufficient representation of the local interactions in areas of extreme densities. In this contribution, we extend the repulsive force term of the social force model to reproduce crowd turbulence. We perform numerical simulations of pedestrians moving through a bottleneck area with this model. The transitions from laminar to stop-and-go and turbulent flows are observed. The empirical features characterizing crowd turbulence, such as the structure function and the probability density function of velocity increments, are reproduced well; i.e., they are well compatible with an analysis of video data during the annual Muslim pilgrimage.

DOI: 10.1103/PhysRevE.76.046105 PACS number(s): 89.40.−a, 45.70.Vn, 47.27.−i, 05.70.Fh

I. INTRODUCTION

Pedestrian dynamics [1–3] has been described by physicists through various macroscopic and microscopic models. Macroscopic models, predominantly fluid-dynamic models [4,5], have the advantage of describing the large-scale dynamics of crowds, especially depicting intermittent flows and stop-and-go flows. These features are basically understood as the effect of a hybrid continuity [6] with two regimes: forward pedestrian motion and backward gap propagation. Details of pedestrian interactions are neglected in these models. In contrast, microscopic models can be used to describe the details of pedestrian behavior. Previously proposed pedestrian models include many-particle force models [7,8], computer-aided (CA) models [9,10], and others—e.g., multiagent approaches [11]—which have received increasing attention among physicists in the past. In recent years, interest has turned to empirical or experimental studies [12–18] of pedestrian flows based on video analysis [1,13,17,19,20]. This has contributed to the calibration of current models [21,22] and the discovery of new phenomena such as crowd turbulence [1], which can help to understand many crowd disasters.

Turbulent motion of pedestrians occurs when the crowd is extremely compressed and people attempt to gain space by pushing others, which leads to irregular displacements or even the falling of people. If the fallen pedestrians do not manage to stand up quickly enough, they will become obstacles and cause others to fall as well. Such dynamics can eventually spread over a large area and result in a crowd disaster.

However, crowd turbulence is not well reproduced and understood by pedestrian models yet, which challenges current many-particle models. Their shortcoming is due to an underestimation of the local interactions triggered by high densities. In the following sections, we will extend the repulsive force of the social force model [3,7,15], which has successfully depicted many observed self-organized phenomena, such as lane formation in counterflows and oscillatory flows at bottlenecks [23].

II. MODEL OF CROWD TURBULENCE

Previous empirical studies [1,24] have revealed that people are involuntarily moved when they are densely packed, and as a consequence, interactions increase in areas of extreme densities, which leads to an instability of pedestrian flows. When the average density is increasing, sudden transitions from laminar to stop-and-go and turbulent flows are observed. Moreover, the average flow does not reach zero. We will now show how turbulent flows can be modeled by a small extension of the social force model [3,7,15]. What we do is to add an extra term to the repulsive force and show how this will give qualitatively different dynamics, leading to turbulent flows.

The social force model assumes that a pedestrian i tries to move in a desired direction $\vec{e}_i$ with desired speed v_i^0 and adapt the actual velocity $\vec{v}_i$ to the desired velocity $v_i^0\vec{e}_i$ within the relaxation time τ. The velocity $\vec{v}_i = d\vec{r}_i/dt$—i.e., the temporal change of the position $\vec{r}_i$—is also affected by repulsive forces.

The social force model is given by

$$m_i \frac{d\vec{v}_i(t)}{dt} = \vec{f}_i(t), \tag{1}$$

where $\vec{f}_i(t)$ is the acceleration force of pedestrian i:

$$\vec{f}_i(t) = m_i \frac{1}{\tau}(v_i^0\vec{e}_i - \vec{v}_i) + \sum_{j(\neq i)} \vec{f}_{ij}(t). \tag{2}$$

The term $\vec{f}_{ij}(t)$ denotes the repulsive force, which represents both the attempt of pedestrian i to keep a certain safety distance from other pedestrians j and the desire to gain more space in very crowded situations.

Instead of introducing an additional force term, one may reflect the desire to gain more space under crowded conditions by a local interaction range in the repulsive pedestrian force $\vec{f}_{ij}$, which is proposed as follows:

$$\vec{f}_{ij} = F\Theta(\varphi_{ij})\exp[-d_{ij}/D_0 + (D_1/d_{ij})^k]\vec{e}_{ij}, \quad (3)$$

where F is the maximum repulsive force (assuming there is no overlap and compression); d_{ij} is the distance between center of masses of pedestrians; k, D_0, and D_1 are constants; $\vec{e}_{ij}$ is the normalized vector pointing from pedestrian j to pedestrian i; and φ_{ij} is the angle between $\vec{e}_{ji}$ and the desired walking direction $\vec{e}_i$ of pedestrian i—i.e., $\cos(\varphi_{ij}) = \vec{e}_i \cdot \vec{e}_{ji}$.

In normal situations, the function $\Theta(\varphi_{ij})$ reflects the fact that pedestrians react much more strongly to what happens in front of them, and it has been suggested [23] to have the form

$$\Theta(\varphi) = \left(\lambda + (1-\lambda)\frac{1+\cos(\varphi)}{2}\right). \quad (4)$$

Also note that when d_{ij} is very small, i.e., people are squeezed, the repulsive force will increase greatly, which reflects the strong reactions of those located in extremely dense areas.

In the original social force model, the second repulsion term $kg(r_{ij}-d_{ij})$ [7] reflects the physical contacts of pedestrians, which will separate pedestrians, when collisions occur. Here k is a constant and the function $g(x)$ is zero if pedestrians do not touch each other; otherwise, it is equal to the argument x. In highly dense areas, the speeds of pedestrians are very low, so the small fluctuations of d_{ij} may not lead to sufficient forces for the occurrence of turbulence, since this repulsive force is increased linearly. Suppose that pedestrian i is located in an extremely dense area. For the extended model, the small fluctuations of d_{ij} will change the repulsive forces greatly and lead to sudden involuntary displacements. With the influence of such strong reactions, the motion of pedestrians near i will be affected and will further spread the irregular displacements to a larger area. Thus the turbulent motion of pedestrians will be triggered.

III. RESULTS AND DISCUSSION

Numerical simulations (supplementary videos [25]) will now be carried out of a crowd going through a bottleneck. The simulations will be performed with the extended-social-force model described in Sec. II.

In our simulations, the desired speeds v^0 are assumed to be Gaussian distributed with mean value $v^0 = 1.34$ m/s and standard deviation 0.26 m/s [26–28]. The relaxation time τ is set to 0.5 s. The average mass of a pedestrian is set to 60 kg with a standard deviation of 10 kg. Assuming that pedestrians have a strong desire to gain more space in dense areas, the maximum repulsive force F is set to 160 N. Note that when pedestrians are compressed, the maximum force can be significantly larger than F. The other parameters are set to $\lambda = 0.25$, $k = 2$, $D_0 = 0.31$, and $D_1 = 0.45$.

The bottleneck area (see Fig. 1) contains two pedestrian sources A and B, where A denotes those walking from left to right, while B represents those walking from the bottom and then turning right to join those coming from the left. These two sources give an increasing number of pedestrians in time, since we use both pedestrian sources and periodic boundary conditions. With this scheme we can see how the transition from laminar to turbulent flow occurs when the density is growing. The whole area is 40 m $\times$ 20 m. The reason for this setup is to get a situation that is comparable to the one in the empirical study [1].

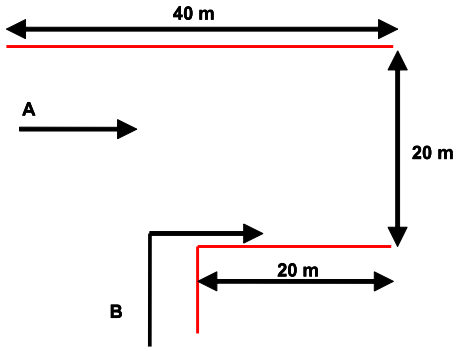

FIG. 1. (Color online) The bottleneck area of the simulation. Two groups of people set out, respectively, from A and B and intersect, causing pedestrians to be highly compressed, which eventually results in turbulent flows.

The preferred direction is defined as follows: If the vertical position of a pedestrian is above the corner, she will walk in the right direction. Otherwise, she will first walk upwards until she is above the corner and then turn to the right and keep walking straight ahead.

Note that interactions increase greatly when those two crowds intersect, especially in high-density situations.

The "crowd pressure" [1], reflecting the irregular and chaotic motion of people, is given by

$$p = \rho_i \mathrm{Var}(\vec{v}_i), \quad (5)$$

where $\mathrm{Var}(\vec{v}_i)$ is the local velocity variance. The local density

$$\rho_i = \sum_j \frac{1}{\pi R^2} \exp[-\|\vec{r}_j(t) - \vec{r}_i(t)\|^2/R^2], \quad (6)$$

where R is a parameter reflecting the range of smoothing. For further aspects regarding the definition of the local density and pressure, see Ref. [1].

The pressure stays low during an increasing density until a point where the pressure suddenly peaks, which leads to turbulent crowd motion (see Fig. 2).

The fundamental diagram (see Fig. 3) demonstrates the effect of the extended repulsive force term. One can clearly see the difference at the tail of the curve, where the flow remains finite with an increase of local density. Note that the flow here is not reduced to zero, even if the density is very high due to the strong interactions within the crowd, which will prevent people from stopping. If the flow is reduced to zero, which means all people stop moving, then there is no turbulence. Therefore it is essential to have nonvanishing flow for high densities. This is compatible with the empirical study [1]. Note that, at this point, the flow is no longer laminar. Therefore, the strong interactions between pedestrians are potentially more dangerous for the crowd. The motion of

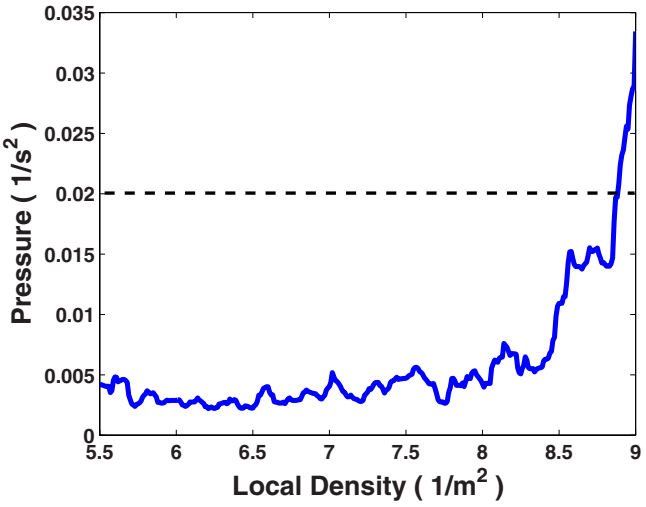

FIG. 2. (Color online) The crowd pressure as a function of local density. The turbulence starts when the pressure exceeds a value of $0.02/s^2$ [1].

pedestrians become turbulent, and people are pushed into all possible directions. As people are pushed by those behind, the fallen people will be trampled if they do not get back on their feet quickly enough. However, in our simulations, we assume that pedestrians will never fall, since we are focusing on the dynamics of the crowd during a high level of crowdedness. These conditions can potentially lead to an accident, but we do not focus on the dynamics of the accident itself.

With the increment of density, the pedestrian flow suddenly turns into stop-and-go flow (see Fig. 4), which is characterized by temporarily interrupted and longitudinally unstable flow. This phenomenon is also predicted by a recent theoretical approach [6], which suggests that intermittent flows at bottlenecks can be triggered when the inflow exceeds the outflow.

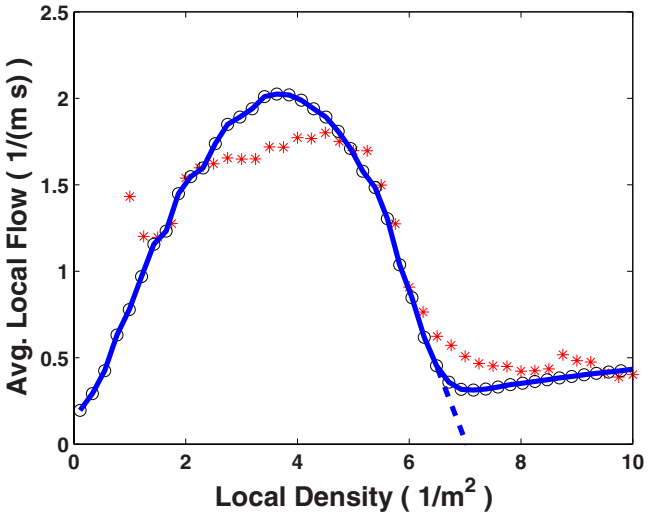

FIG. 3. (Color online) The average of the local flow [1] as a function of the local density. The empirical data are represented by stars, and the simulation results are represented by circles connected by a solid line. The dashed line shows the fundamental diagram from the original social force model.

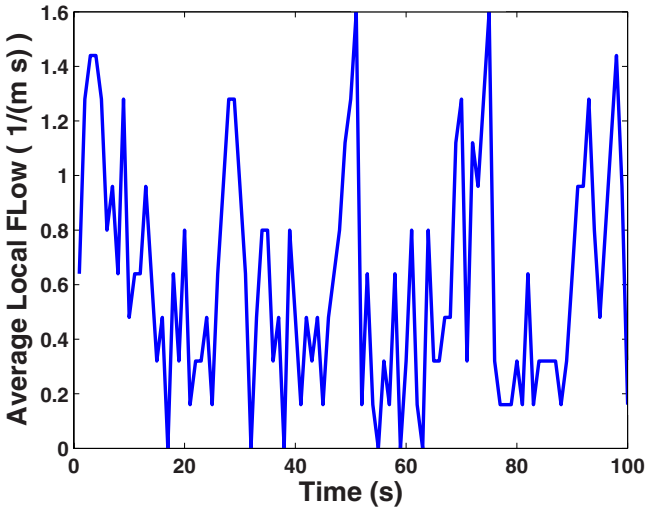

FIG. 4. (Color online) Simulation results. During high crowd densities, the smooth, laminar flow will turn into stop-and-go flow. Here the average density is $4.3/m^2$.

Further increment of the density will lead to turbulent flows. Figure 5(a) shows a typical trajectory of the turbulent motion from our simulations. We can see that, first, the curve is smooth, which represents a laminar flow; then suddenly, vibrations occur due to the turbulence. Also, note that the pedestrian is sometimes even pushed backward. The turbulent motion does not vanish until an individual walks out of the extremely dense central area, where the two streams intersect. Figure 5(b) is an example of the temporal evolution of an individual's velocity components v_y and v_x. One can clearly see the irregular motion into all directions. Although no large eddies are observed, as in turbulent fluids, there is still an analogy to the turbulence of the currency exchange market [29]. This can be characterized by the probability density function of velocity increments and the so-called structure function, Eq. (8).

The shape of the probability density function of the velocity increment is a typical indicator of turbulence if the time shift τ' is small enough and is given by

$$v_x^{\tau'} = v_x(\vec{r}, t + \tau') - v_x(\vec{r}, t). \tag{7}$$

The structure function

$$S(\Delta\vec{r}) = \langle \| \vec{v}(\vec{r} + \Delta\vec{r}, t) - \vec{v}(\vec{r}) \|^2 \rangle_{\vec{r},t} \tag{8}$$

reflects the dependence of the relative speed on the distance.

We find that the probability function of the velocity increment is sharply peaked for turbulence, while it is parabolic-like for laminar flow (see Fig. 6) when the time shift τ' is small enough. The structure function has a slope of 2.0 when the distance is small, while at large steps, the slope turns to 0.18 due to the increased interactions in crowded regions. Both functions are compatible with an analysis of video recordings of the Jamarat Bridge [1].

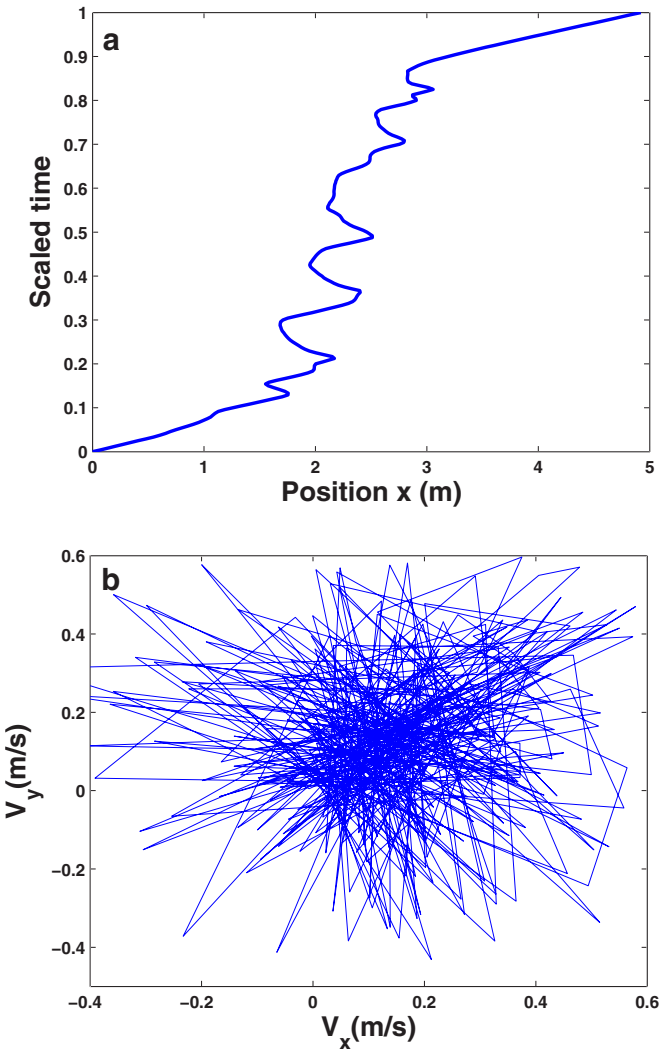

FIG. 5. (Color online) (a) A representative pedestrian trajectory in laminar and turbulent flow. (b) An example of velocity components in the turbulent motion. Here the average density is $9.0/\mathrm{m}^2$.

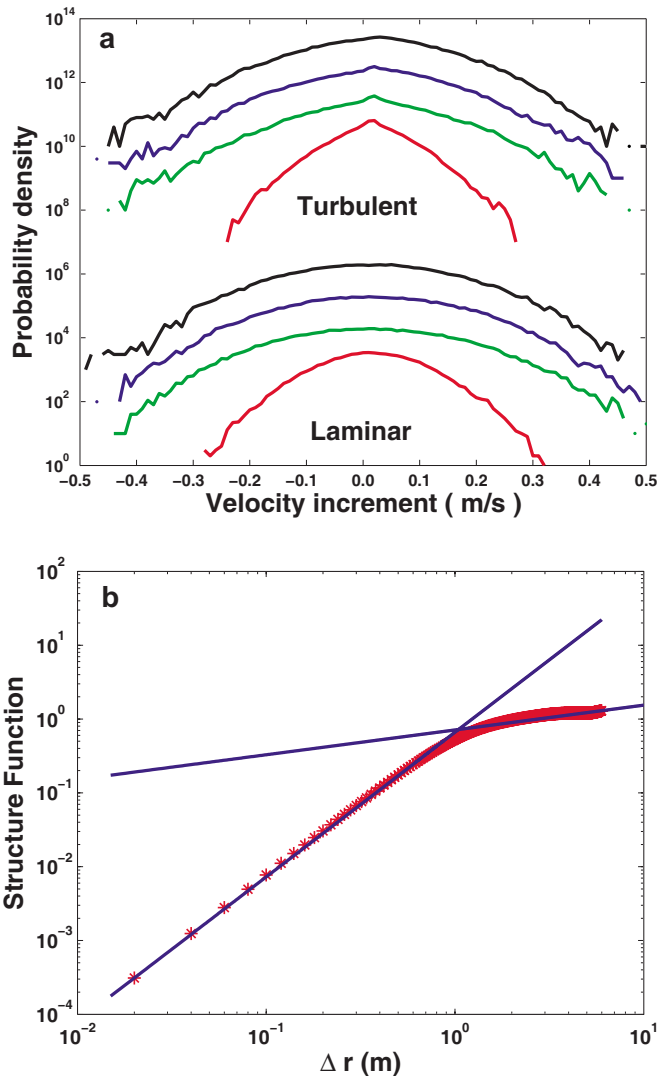

FIG. 6. (Color online) (a) the probability density function of the velocity increment in the laminar and turbulent regions, determined over many locations $\vec{r}$ for $R=\sqrt{10/\rho}$ and $\tau'=2$ s (black curves, top), $\tau'=1$ s (blue curves, second), $\tau'=0.5$ s (green curves, third), and $\tau'=0.05$ s (red curves, bottom). For clarity of presentation, the curves are shifted in the vertical direction. The nonparabolic, peaked curve for small values of τ' distinguishes turbulence from laminar flows. (b) The log-log plot of the structure function for crowd turbulence. The average density here is $9.0/\mathrm{m}^2$.

IV. SUMMARY AND OUTLOOK

In summary, an added social force component, reflecting the strong interactions in the extremely crowded areas, is proposed for the simulation of crowd turbulence, which questions current many-particle models. The transition from laminar to stop-and-go and turbulent flows is observed in the simulations. The fundamental diagram is reproduced and demonstrates the effects of the extended repulsive forces in highly dense situations; i.e., the average local flow is not reduced to zero. A typical turbulent trajectory and velocity components are presented. Functions like the probability density function of the velocity increment and the structure function, characterizing the features of turbulence are simulated, and the results are compatible with empirical studies.

ACKNOWLEDGMENT

The authors are grateful to the German Research Foundation for funding (DFG Project No. He 2789/7-1), and to thank Dirk Helbing for giving valuable input to this study.

[1] D. Helbing, A. Johansson, and H. Z. Al-Abideen, Phys. Rev. E **75**, 046109 (2007).
[2] K. Still, Ph.D. thesis, University of Warwick, 2000 (unpublished).
[3] D. Helbing and P. Molnar, Phys. Rev. E **51**, 4282 (1995).
[4] R. L. Hughes, **35**, 169 (2003).
[5] R. L. Hughes, Transp. Res., Part B: Methodol. **36**, 507 (2002).
[6] D. Helbing, A. Johansson, J. Mathiesen, M. H. Jensen, and A. Hansen, Phys. Rev. Lett. **97**, 168001 (2006).
[7] D. Helbing, I. Farkas, and T. Vicsek, Nature (London) **407**, 487 (2000).
[8] W. J. Yu, R. Chen, L. Y. Dong, and S. Q. Dai, Phys. Rev. E **72**, 026112 (2005).
[9] M. Muramatsu and T. Nagatani, Physica A **275**, 281 (2000).
[10] C. Burstedde, K. Klauck, A. Schadschneider, and J. Zittartz, Physica A **295**, 507 (2001).
[11] A. Willis, R. Kukla, J. Hine, and J. Kerridge (unpublished).
[12] D. Helbing, M. Isobe, T. Nagatani, and K. Takimoto, Phys. Rev. E **67**, 067101 (2003).
[13] W. Daamen and S. P. Hoogendoorn, in *Proceedings of the 82nd Annual Meeting at the Transportation Research Board*, (Transportation Research Board, Washington, DC, 2003), pp. 20–30.
[14] M. Isobe, D. Helbing, and T. Nagatani, Phys. Rev. E **69**, 066132 (2004).
[15] D. Helbing, L. Buzna, A. Johansson, and T. Werner, Transport. Sci. **39**(1), 1 (2005).
[16] A. Seyfried, B. Steffen, W. Klingsch, and M. Boltes, J. Stat. Mech.: Theory Exp. (2005) P10002.
[17] T. Kretz, A. Grünebohm, and M. Schreckenberg, J. Stat. Mech.: Theory Exp. (2006) P10014.
[18] A. Seyfried, T. Rupprecht, O. Passon, B. Steffen, W. Klingsch, and M. Boltes, e-print arXiv:physics/0702004.
[19] K. Teknomo, Ph.D. thesis, Tohoku University Japan, Sendai, 2002 (unpublished).
[20] J. Kerridge, S. Keller, T. Chamberlain, and N. Sumpter, in *Pedestrian and Evacuation Dynamics 2005*, edited by N. Waldau *et al.* (Springer-Verlag, Berlin, 2007), pp. 27–39.
[21] A. Johansson, D. Helbing, and P. K. Shukla, Adv. Complex Syst. (to be published).
[22] S. P. Hoogendoorn, W. Daamen, and R. Landman, in *Pedestrian and Evacuation Dynamics 2005*, edited by N. Waldau *et al.* (Springer-Verlag, Berlin, 2007), pp. 253–265.
[23] D. Helbing, I. Farkas, P. Molnar, and T. Vicsek, in *Pedestrian and Evacuation Dynamics*, edited by M. Schreckenberg and S. D. Sharma (Springer, Berlin, 2002), pp. 19–58.
[24] J. J. Fruin, in *Engineering for Crowd Safety*, edited by R. A. Smith and J. F. Dickie (Elsevier, Amsterdam, 1993), p. 99.
[25] Supplementary videos are available at http://www.trafficforum.org/turbulence_sim
[26] L. F. Henderson, Nature (London) **229**, 381 (1971).
[27] F. P. D. Navin and R. J. Wheeler, Traffic Eng. **39**, 30 (1969).
[28] U. Weidmann, *Transporttechnik der Fußgänger, Schriftenreihe des Instituts für Verkehrsplanung*, Transporttechnik, Straßen- und Eisenbahnbau, No. 90 (ETH-Zürich, Zürich, 1993), pp. 87–88.
[29] S. Ghashghaie, W. Breymann, J. Peinke, P. Talkner, and Y. Dodge, Nature (London) **381**, 767 (1996).